

New *Phytologist* Supporting Information

Article title: CsiLAC4 modulates boron flow in *Arabidopsis* and *Citrus* via high-boron-dependent lignification of cell walls

Authors: Jing-Hao Huang, Ling-Yuan Zhang, Xiong-Jie Lin, Yuan Gao, Jiang Zhang, Wei-Lin Huang, Daqiu Zhao, Rhuanito Soranz Ferrarezi, Guo-Cheng Fan, Li-Song Chen

Article acceptance date: 03 November 2021

The following Supporting Information is available for this article:

Fig. S1 Information of the pBI121 vector

Fig. S2 Alignment of CsiLAC4 and CsiLAC17

Fig. S3 Topology of CsiLAC4 and CsiLAC17

Fig. S4 Subcellular localization of CsiLAC4 and CsiLAC17

Fig. S5 Phylogenetic analysis of CsiLAC17

Fig. S6 Lignin contents of transgenic *Arabidopsis*

Fig. S7 Effects of boric acid and NaCl supplements on hypocotyl growth

Fig. S8 Boric acid excess stimulates early flowering in the CsiLAC4^{OE} lines

Fig. S9 Effects of boric acid excess on hypocotyl anatomy

Fig. S10 Effects of boric acid treatments on gene expression in *Arabidopsis*

Fig. S11 Melting curves of genes tested in this study

Fig. S12 Effects of boric acid excess on interfascicular fiber thickness in the CsiLAC4^{OE} lines

Fig. S13 Expression of LACCASE-like family genes in boric acid-treated *Citrus* leaves

Fig. S14 Effects of boric acid excess on the nutrient accumulation in *Arabidopsis*

Table S1 Primers for PCR cloning and hybridization

Table S2 Primers for site-directed mutagenesis

Table S3 miRNA northern blotting probe

Table S4 Specific and nested primers for 5'-RACE PCR

Table S5 Primers for RT-PCR of LACCASE-like family genes

Table S6 Boron fractions in *Citrus* leaves treated with different boric acid treatments

Fig. S1 Information of the pBI121 vector

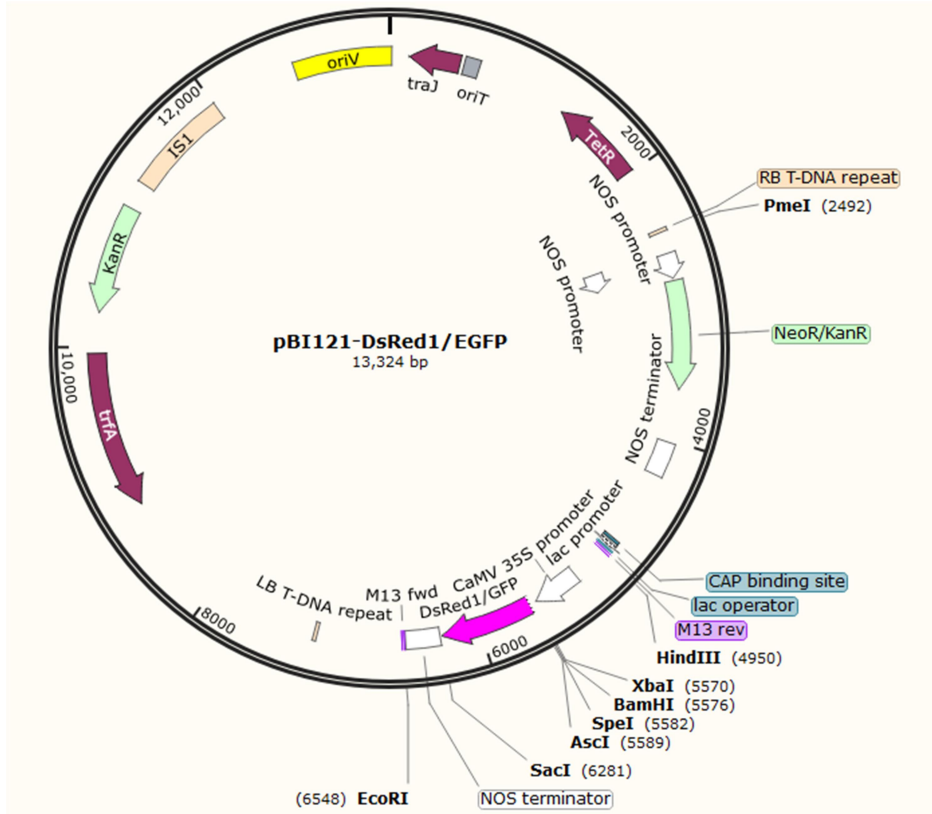


Fig. S2 Alignment of CsiLAC4 and CsiLAC17. A BLAST search of the *Citrus* genomic database (<http://citrus.hzau.edu.cn/cgi-bin/orange/blast>) displayed that CsiLAC4 (Cs6g07800, from *C. sinensis*) shares 99.94% identity with CgiLAC4 (Cg6g006410.1, from *C. grandis*) and that CsiLAC17 (Cs8g17630) shares 99.77% identity with CgiLAC17 (Cg8g021370.1). Therefore, we used only CsiLAC4 and CsiLAC17 for the subsequent studies. Blue lines indicate signal peptides predicted by the SignalP v5.0 program (<http://www.cbs.dtu.dk/services/SignalP>).

AtLACCASE-4	MGSHMWFLELVSVFFSVPFAPSSESMVRHYKFNVMKNTLRCSSKHTVTVNGRYPGPTLYAREDDTLIKVVNHVKYVSIHWHGVQRVRTGWADGPAYI	100
CsiLAC4	MDSWVRLHLLVAACL..FPALVECRVRYKFNVMKNSLRLCSSKHITVTVNGKFPGPTLYAREDDTLIKVVNHVKYVSIHWHGVQRVRTGWADGPAYI	97
Consensus	m s v l lv fpa e vrhykfnvmkn t lcsskp vtvng pgpt yare dt l kvvnhvkvyn ihwhgvqr rtgwadgpayi	
AtLACCASE-4	TQCPIQSGOVVYNYLITGQRGTLWHAHILWLRATVHGALVILPKRGVPPYFPKEDNEKVTIVLGEWWSKSDTENIINCAIKSLGAPNVSDSHMINGHPGP	200
CsiLAC4	TQCPIQSGHSIVYNYLITGQRGTLWHAHILWLRATVHGATVILPKRGVPPYFPKEDNEKVTIVLGEWWSKSDTEAVINCAIKSLGAPNVSDSHMINGCPGPE	197
Consensus	tqcpiq g y yn t t gqrgtl whahilwlratv ga vilpkrgvppypfpk e v vl ewwksdte in al sglapnvdsdh ing pgp	
AtLACCASE-4	VRNCPSCQYRLSWENKTYLLRLVNAALNEELFFKTAGHIFTVVEVDAYVVKPFKTDIIVLAPGQTTNVLITASKSAGKYLVTASPFMDAPIAVDNVTA	299
CsiLAC4	ISSCSQCGFTLFWDSCKTYMLRIINAALNEELFFKTAGHIFTVVEVDATVVKPFKTDIIVLAPGQTTNVLISAKTSCKYLVAASPFMDAPIAVDNATA	297
Consensus	c sqg l v gkty lr naalneelffk agh tvvevda yvkpfktdt iapgqttnvll a k gkylv aspfmdapiavdn ta	
AtLACCASE-4	TATVHYSGLTSSSEPTLLTLPFPPNATSIANNFTINSLRSLNSKKYPALVPTIIDHHLFFTVGLGNAFCPTCKAGNGSRVVASINNVTFIMEKTALLFAHMF	399
CsiLAC4	TATLHYSGLTASSATLLTSTPEKNGTATANKFTIDSLRSLNSKKYPARVPTVDHNLFFTVGLGVNFCPSCKAGNGSRVVASINNVTFVMEPTIALLCAHFF	397
Consensus	tat hysgtl ss t lt pp n t ian f slrslnskkypa vp t dh l ftvglg n cp ckagnsrrvasinnvtf mp all ah f	
AtLACCASE-4	NISGVFTTDFKPNPPHVFVYSGSSVTMMDETCTRLVYKLFYNAFVQLLQDTCIAPENHPVHLHGFFNFVGRGLGNFNSTKDPKNFNLVDPVERNTIG	499
CsiLAC4	NISGVFTTDFKPNPPHYNFTG.TPKNLQSNCTKAYRLAYNSTVQLLQDTCIAPENHPVHLHGFFNFVGRGLGNFNPKDKPKFNLVDPVERNTIG	496
Consensus	n sgvfttdfp npph n g n t gt y l yn tvql lqdtg iapenhpvhlhgfnff vg glgnfn kdpk fnlvdpverntig	
AtLACCASE-4	VPSGGVWVIRFADNPGVWFMHCHLEVHTTWGLKMAFLVNGKGPNSILPPPSDLPK	557
CsiLAC4	VPSGGVWVIRFADNPGVWFMHCHLEVHTTWGLKMAFLVNGKGPNSILPPPSDLPK	554
Consensus	vpsggvwv irf adnpgvwfmhchlevhttwglkmaflv ngkgn s lppp dlpk	
AtLACCASE-17	...MALQ..LLLAIESCVLLLPQPAFGITRHYTLEIKMONTVRLCHTKSLVSVNGQFPGEKLIAREGQVLIKVVNVVFNISLIHWHGIRQLRSGWADG	94
CsiLAC17	MGASFAIMGFVLLTWLS.LGLLESVLAITRHYKFNVELNVTRLCHTKSLVSVNGQFPGERIVAREGRLIKVVNHVFNISLIHWHGIRQLRSGWADG	99
Consensus	al ll v s llp itrhy nvtrlchtk lsvngqfpgp aregd likvvn v nis hwhgirqlrsgwadg	
AtLACCASE-17	PAYITQCPIQTQGSVYVNYTIVGQRGTLWHAHISWLRSTVYGHILILPKRGVPPYFAKPKKEVFMIFGEWFNADTEALTRQAOTGGGPNVSDAYTING	194
CsiLAC17	PAYITQCPIQTQGSVYVNYTIVGQRGTLWHAHISWLRSTVYGHILILPKRGVPPYFAKPKKEVFMIFGEWFKSDTEAIIINQALOTGGGPNVSDAYTENG	199
Consensus	payitqcpiqtggsyvyn tivgqrgtlw hahiswlrst ygp iilpkrg pyfpakp kevp fgewf dteaii qa qtggpnvsdayt ng	
AtLACCASE-17	LPGLYNCSAKDTEFIRVKEGKTYLLRLINAALNDELFFSIANHTVTVVEADAIVVKPFETETILVAPGQTTNVLITKSSVPSASFFMTARPYVTGCGT	294
CsiLAC17	LPGLYNCSAKDTEFIRVKEGKTYLLRLVNSALNDELFFSIANHTVTVVEADAIVVKPFETETILVAPGQTTNVLITKPHVPSATFFMTARPYATGLGT	299
Consensus	lpglyncsakdtef l vk gktyllrl n alnd lffsianht tvve da yvkpfetet i pgqttnvll tk ypsa ffmtarpy tg gt	
AtLACCASE-17	FDNSTVAGILEYEPKQTKGAHSRTSTKNIOLFEPILBALNDTNEATKFSNKLRSLSNKNFANVPLNVRKFFFTVGLGNTGPNHKNNOTCOGHTNITM	394
CsiLAC17	FDNSTVAGILEYEP...LNFIHSGNSIKKLEFKPILBPLNDTNEATKFSNKLRSLSNKNFANVPLNVRKFFFTVGLGNTGPR..NOTCOGE.NGTM	394
Consensus	fdnstvagileye p hs sik l lfkpilp lndtnf t f nkrls s fpanvp n d ffftvgigt pc nqtqgp n tm	
AtLACCASE-17	FAASISNISHTMPTKALLOSSEYSQSHGVYSKFFVWSEIVPFNYTGNPPNNTMVSNGINLMLVLYNTSVELVMQDTSILGABSHPHLHGFNFVVGQGF	494
CsiLAC17	EPASIDNISHTMPTKALLOSHYSQSHGVYVSEFFVWSEIVPFNYTGNPPNNTMVSNGIKLVLYNTSVELVMQDTSILGABNHPHLHGFNFVVGQGF	494
Consensus	f asi nisf mpt allq h gqs gvy p fp sp pfnytg ppnntmvs gt l vlp ntsvel mqdtsilgae hplhlg nffvvgqgf	
AtLACCASE-17	GNFDPNKDERNFNLVDPPIERTVGVPSGGWVAIRFLADNPGVWFMHCHLEVHTSWGLRMAWLVLDGDRFDQKLLPPPADLPK	576
CsiLAC17	GNFDPNKDAKFNLVDPPIERTVGVPSGGWVAIRFLADNPGVWFMHCHLEVHTSWGLKTAWLVLDGKFNQKLLPPPADLPK	576
Consensus	gnfdpnkdp fnlvdpiertvgvpsggw airfladnpgvwfmhchlevhtswgl awlvldg p qllpppadlpk	

Fig. S3 Topology of CsiLAC4 (a) and CsiLAC17 (b). Signal peptide and transmembrane topology were predicted with online software Pobius (<http://phobius.sbc.su.se/index.html>). None of the transmembrane domains could be found by the online software SOSUI (<http://harrier.nagahama-i-bio.ac.jp/sosui>). Red lines indicate signal peptides; blue lines display non-cytoplasmic peptides, while green lines indicate cytoplasmic peptides.

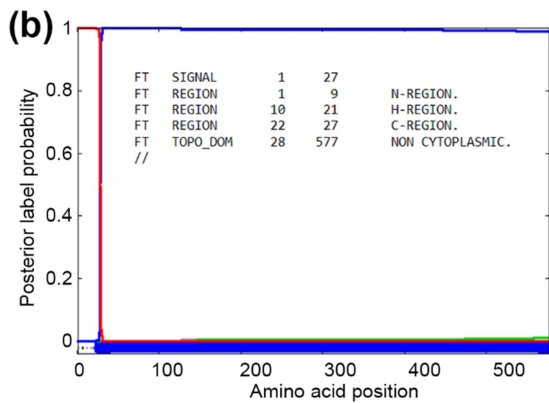
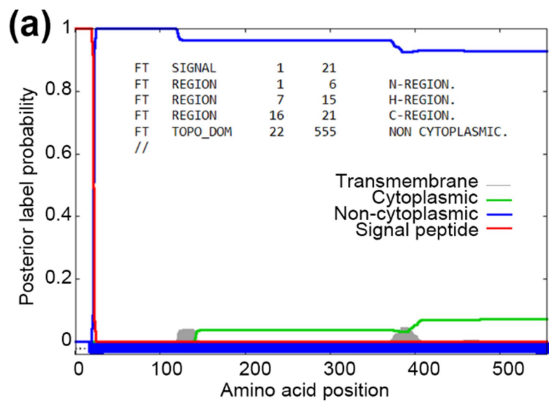


Fig. S4 Subcellular localization of CsiLAC4 and CsiLAC17. CsiLAC4-DsRed (g-l) and CsiLAC17-DsRed (m-r) were transiently introduced into tobacco epidermal cells by *Agrobacterium*-mediated transfection. GFP was co-transfected and used as a protoplasmic marker. (d-f, j-l and p-r) Leaf blades were plasmolyzed with 0.8 M sorbitol before being subjected to microscopy. The fluorescence signal was detected 72h post-transfection. White arrows indicate the apoplastic signals. Bars, 90 μ m.

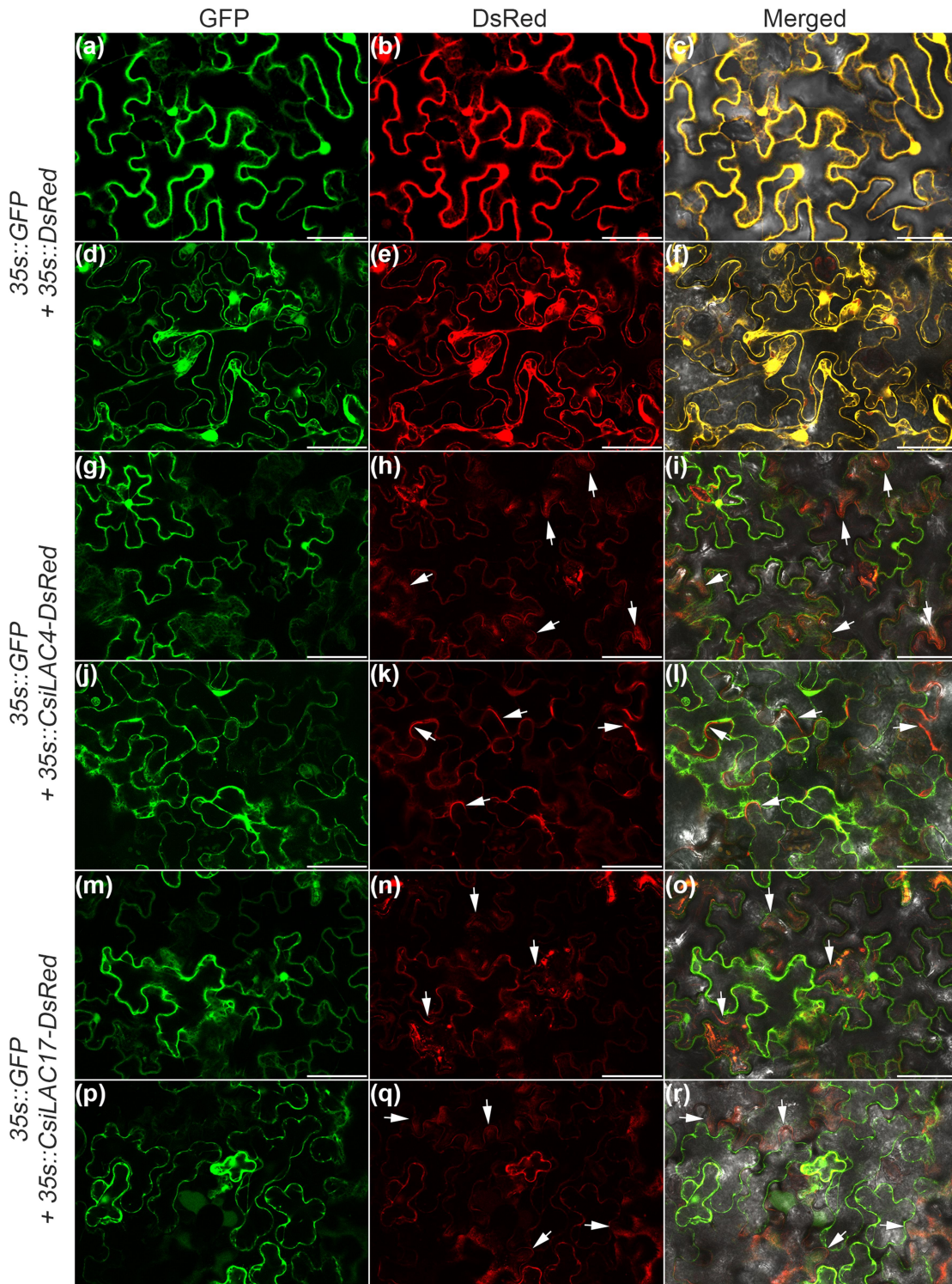


Fig. S5 Phylogenetic analysis of CsiLAC17. Multiple alignments were performed using the ClustalW tool of MEGA7 (<https://www.megasoftware.net/>). An unrooted phylogenetic tree was then constructed using MEGA7 (Neighbor-Joining method with 1000 bootstrap test). The 0.10 scale bar shows substitution distance. LAC17 homologs in woody *C. grandis* and *C. sinensis* and herbaceous plants (*A. thaliana* and *N. tabacum*) are shown.

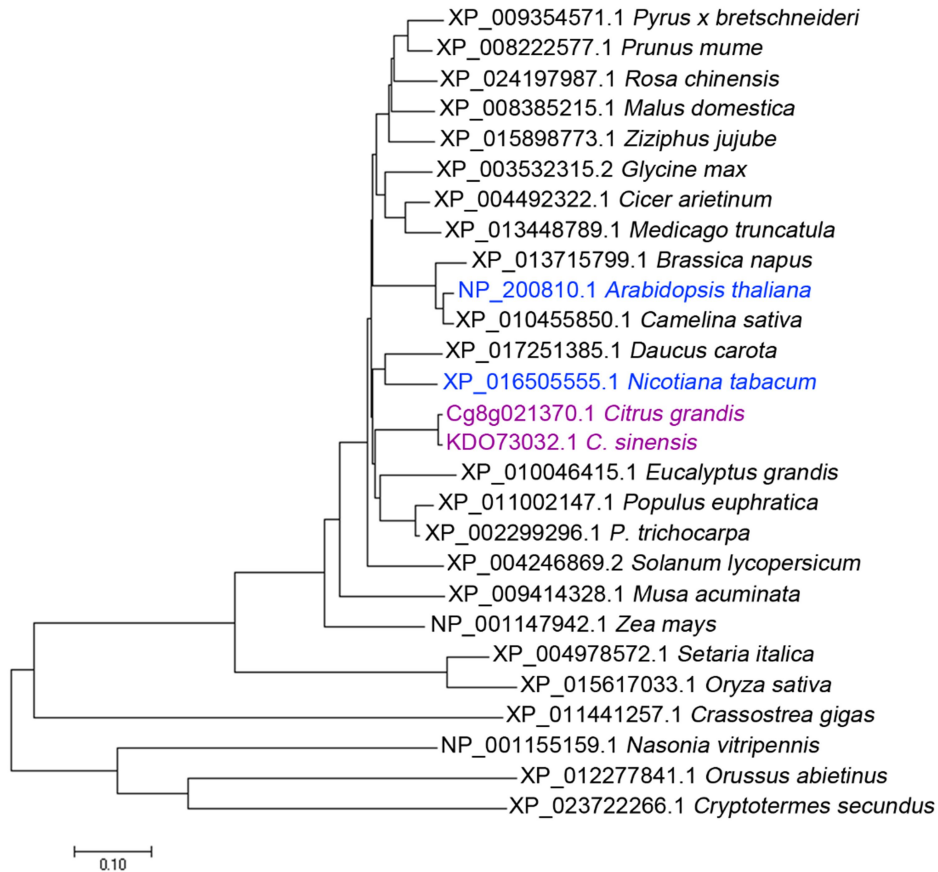


Fig. S6 RT-PCR detection of *CsiLAC4* (a) and *CsiLAC17* (b) and lignin contents (c) in the corresponding transgenic *Arabidopsis* lines. (a-b) Gene expression in shoots was detected from two-week-old T3 seedlings. (c) Rosette leaves and inflorescence stems were dissected from two-month-old T3 plants. Ranges of lignin content are 145.8-155.1, 142.3-150.3, 126.3-157.5 and 126.8-141.3 mg per grand cell-wall material (CWM) in rosette leaf, and 232.6-253.4, 178.9-262.2, 275.5-296.0 and 255.3-295.3 in inflorescence stem for Col-0, miR397^{OE}, CsiLAC4^{OE} and CsiLAC17^{OE} line, respectively. Significant difference are shown at $P < 0.05$ level by One-way ANOVA (S-N-K method, $n = 3$, except for $n = 5$ for miR397^{OE} line)

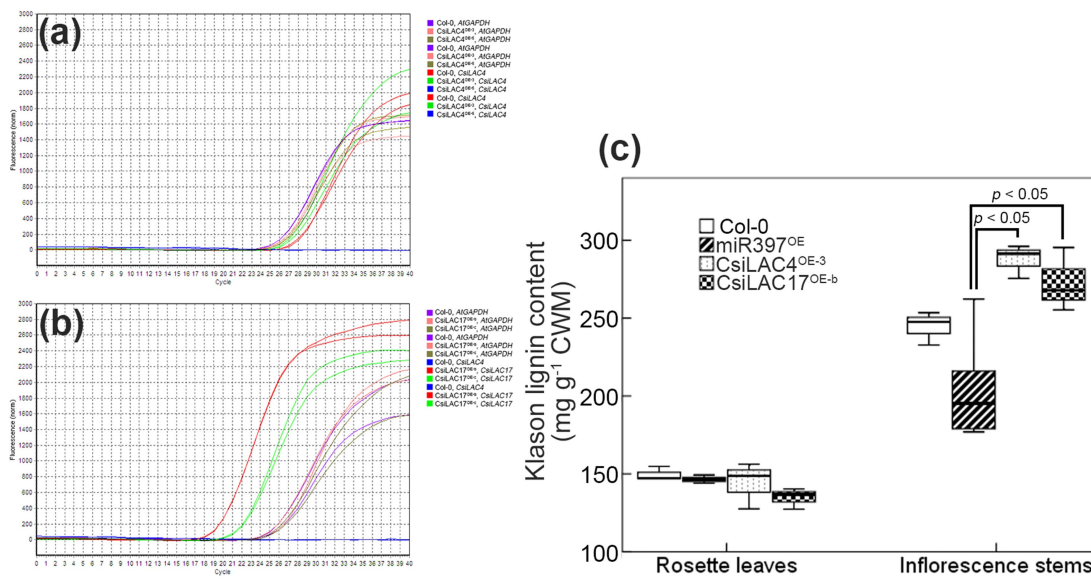


Fig. S7 Supplementation of boric acid (a and b) or NaCl (c and d) significantly increases the hypocotyl length of CsiLAC4^{OE} lines. Vernalized seeds sown on 1/2 MS medium were kept in a chamber under standard culture conditions for 14 days. Hypocotyl length was measured by Image J 1.48 (NIH, USA). (b and d) Results were mean +/- SD. '*' and '**' indicate significant difference at $P < 0.05$ and 0.01 level respectively by One-way ANOVA (S-N-K method, $n = 6$). Bars, 1 cm.

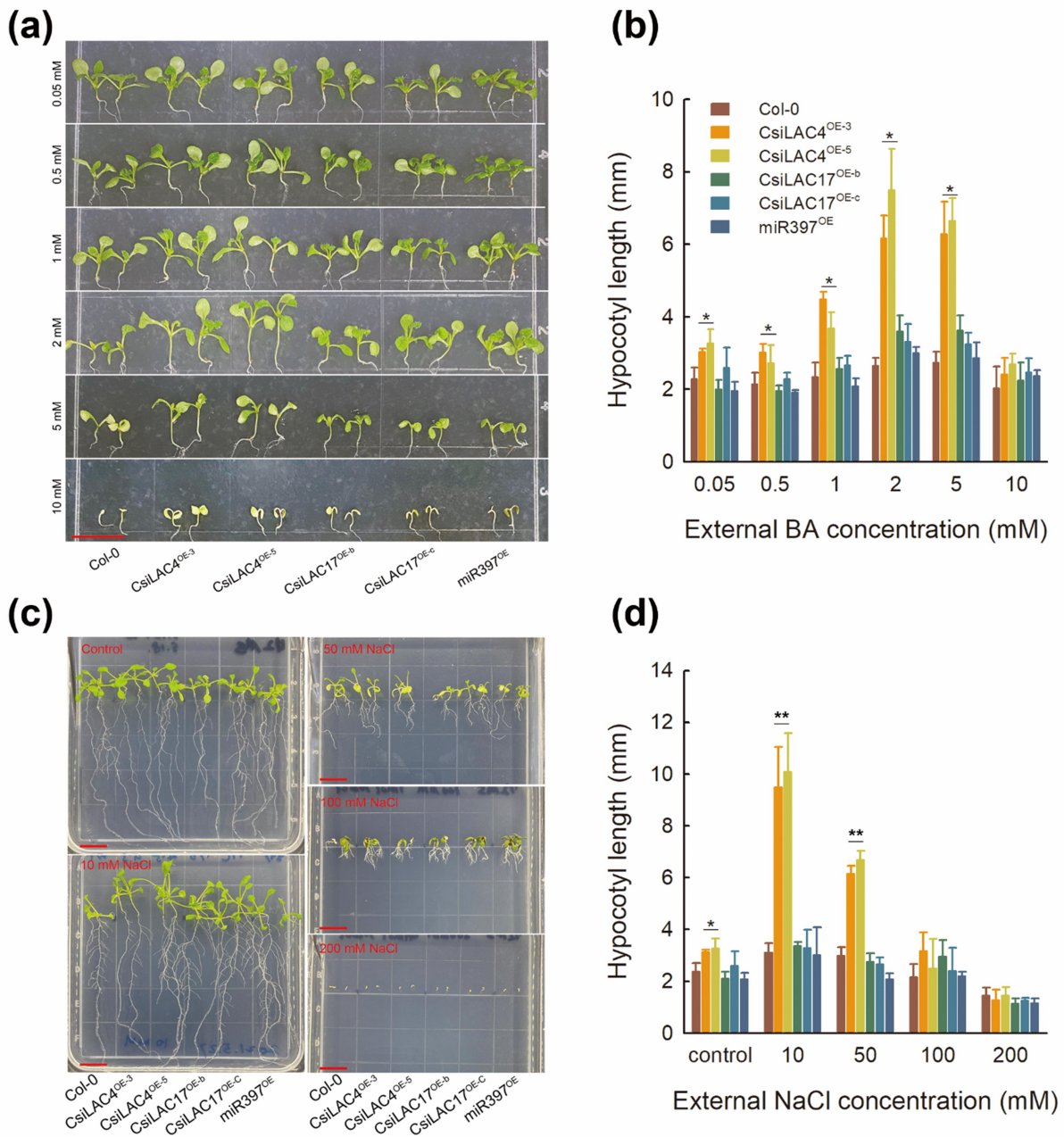


Fig. S8 Boric acid excess advances flowering of the CsiLAC4^{OE} lines. Three-week-old seedlings were irrigated with 1/2 MS liquid medium supplemented with boric acid every other day. Pictures were taken 7 d after the boric acid treatment application.

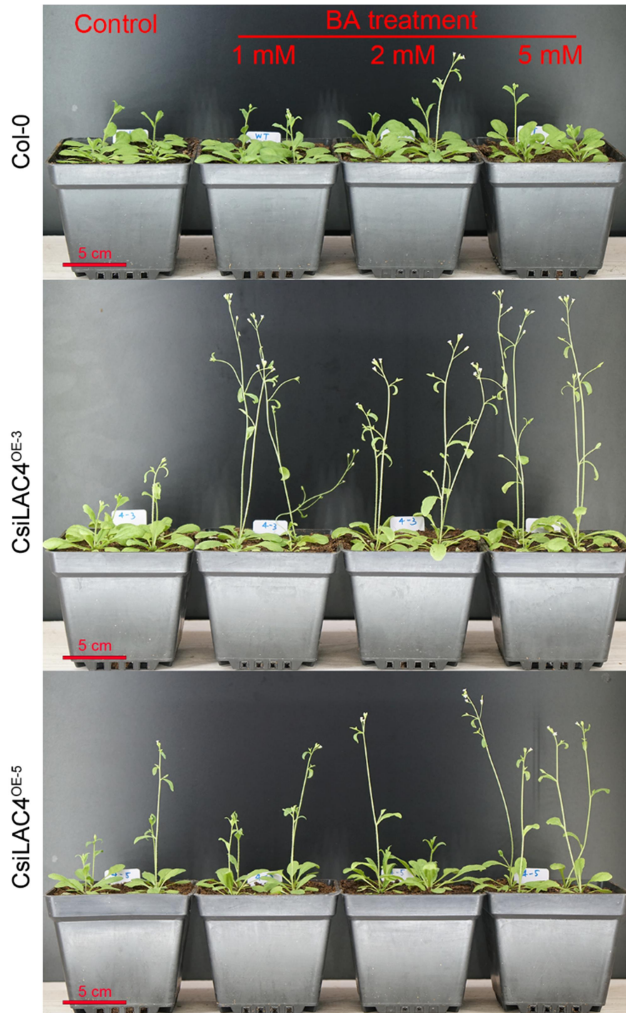


Fig. S9 Boric acid supplementation increased the diameter of metaxylem vessels in the hypocotyl of the CsiLAC4^{OE} line. (a) Transverse paraffin sections from middle hypocotyls were stained with phloroglucinol-HCl. Red arrows indicated the Casparian strip, and double red arrowheads displayed enlarged metaxylem vessels. The number of xylem vessels (b) were calculated and the diameter of metaxylem vessels (c) were determined with the Image J software. Results were mean +/- SD. '*' and '**' indicate significant difference at $P < 0.05$ and 0.01 level respectively by One-way ANOVA (S-N-K method, $n = 4$). Bars, 50 μm .

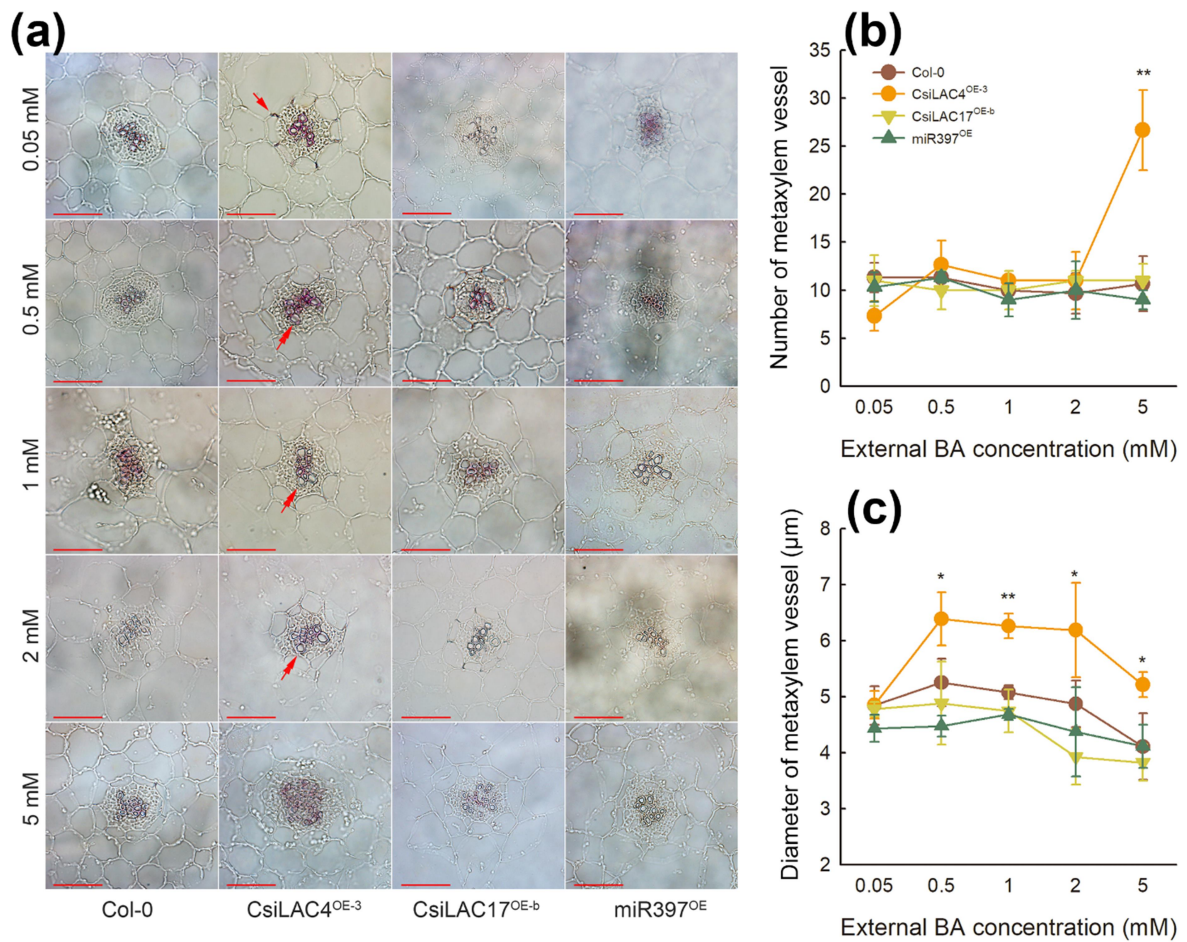


Fig. S10 Relative expressions of *AtLAC4*, *AtLAC17*, *CsiLAC4*, *CsiLAC17* and miR397 in the wild type (Col-0), *CsiLAC4*^{OE}, and *CsiLAC17*^{OE} lines (a and b) and alignment of miR397 of different plant species (c). (a-b) low boric acid level promotes *AtLAC4* and *AtLAC17* expression in all the plant lines; however, both *AtLAC4* and *AtLAC17* expressions are suppressed as external boric acid increases. *AtGAPDH* (a) and *AtUBQ5* (b) were used as internal references. (c) Matured miR397 sequences were obtained from miRBase 22.1 (<http://www.mirbase.org>). *hvu*, *Hordeum vulgare*; *bdi*, *Brachypodium distachyon*; *tcc*, *Theobroma cacao*; *vvi*, *Vitis vinifera*; *csi*, *C. sinensis*; *ath*, *Arabidopsis thaliana*; *nta*, *N. tabacum*.

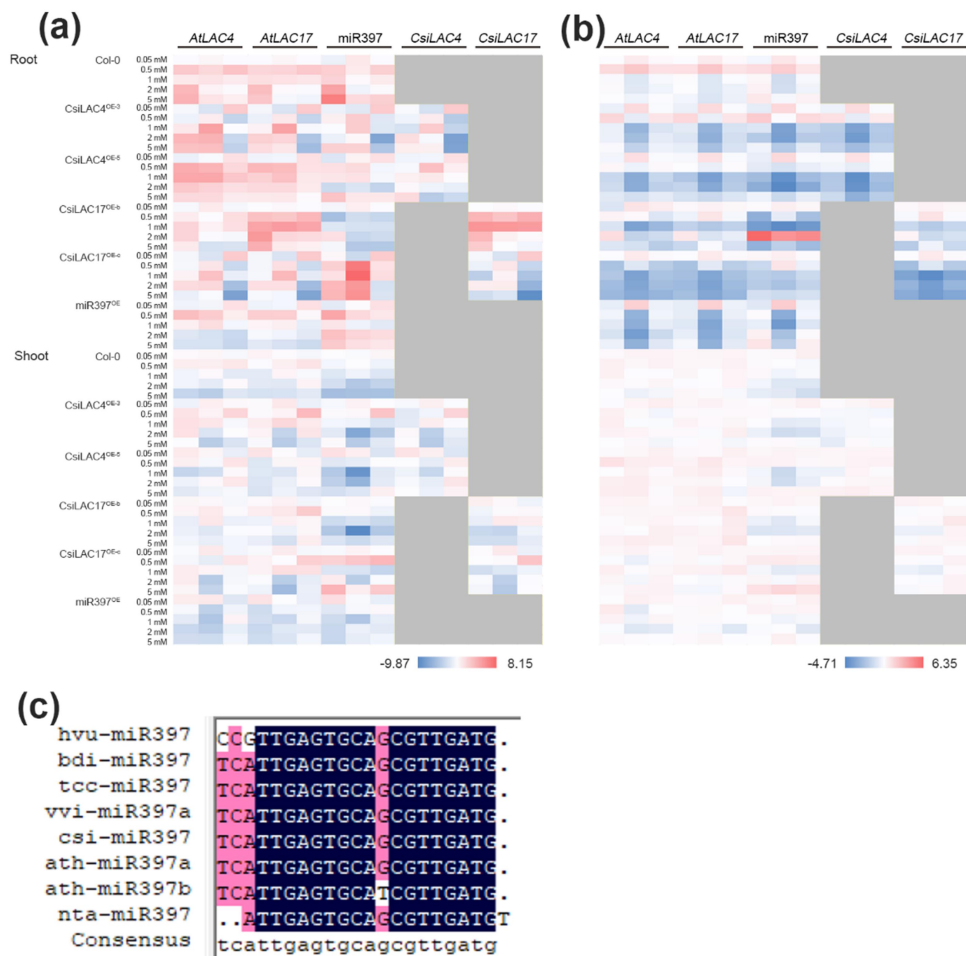


Fig. S11 Melting curves of the laccase-like family members and internal reference genes tested in Fig. S10 and S13.

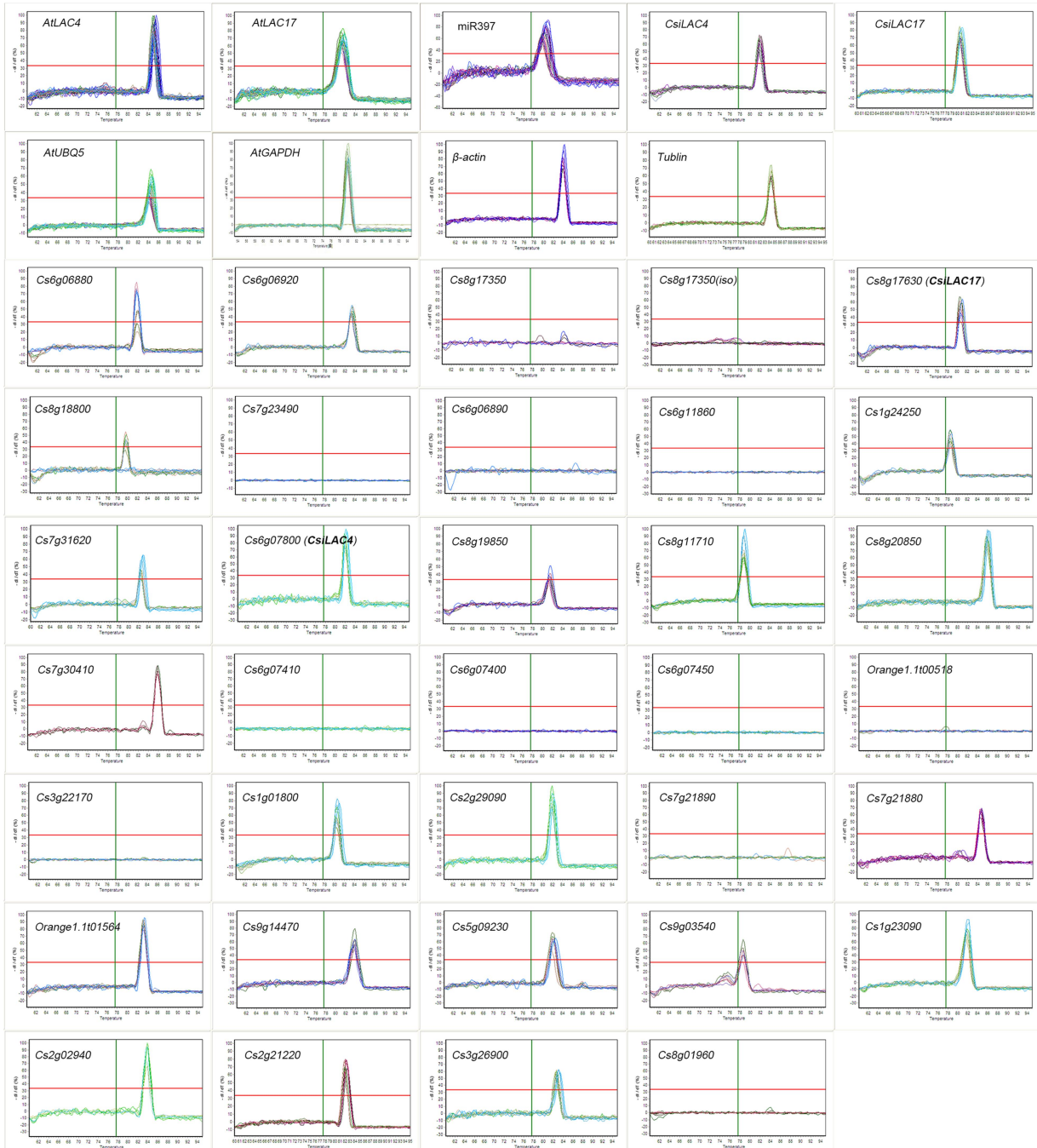


Fig. S12 Boric acid excess increases the thickness of interfascicular fiber (yellow double-arrowheads) in the inflorescence stem of *CsiLAC4*^{OE} lines. Hand sections were cut from mature inflorescence stem (5 cm above the rosette) 14 d post the boric acid treatment and stained with phloroglucinol-HCl. Bars, 100 μ m.

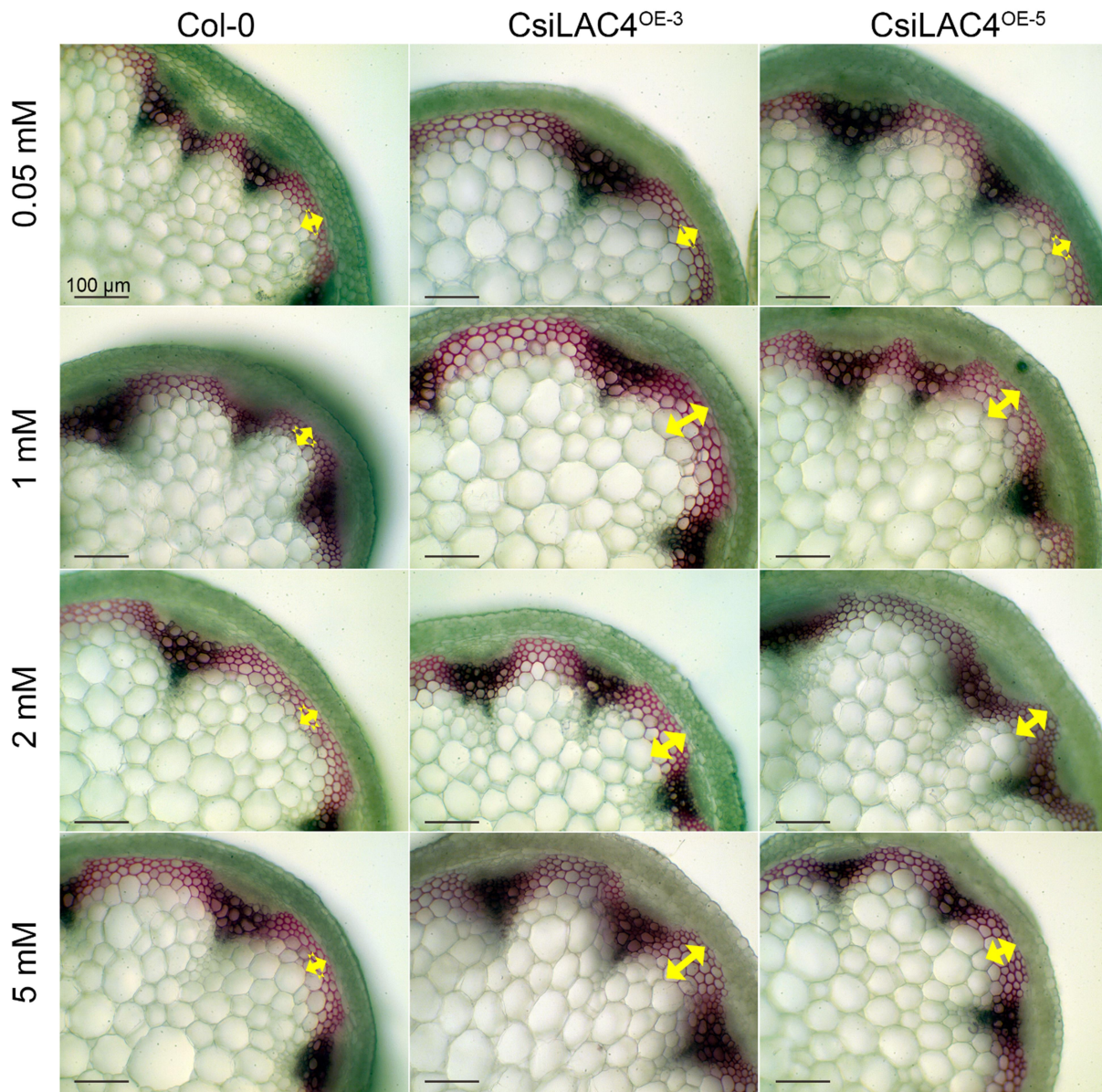


Fig. S13 Bioinformatics analysis of LACCASE-like family members in *Citrus* and their expressions in boric acid-treated leaves. (a) The phylogenetic tree was constructed with MEGA7 software (Maximum-Likelihood method with 1000 bootstrap test). The 0.20 scale bar shows substitution distance. (b-c) Relative levels of genes were expressed as $2^{-\Delta\Delta Ct}$ using β -actin (b) or *Tubulin* (c) as internal control. Results were normalized with Log2 transformation and represented in heatmap using excel software.

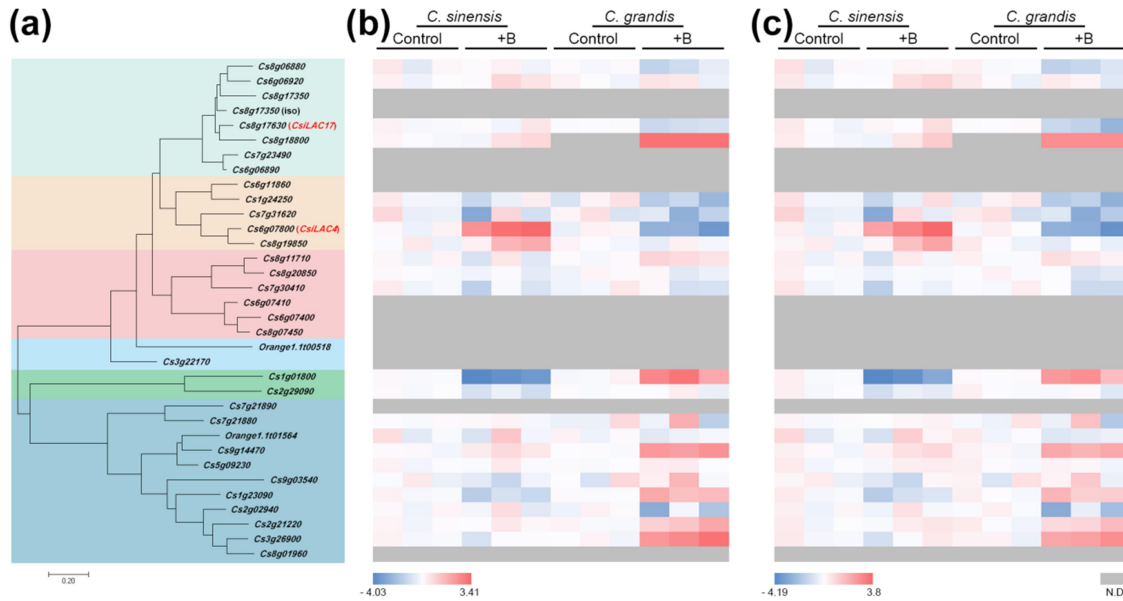


Fig. S14 Nutrient concentration in rosette leaves (a-e, p), roots (f-j, q) and root cell walls (k-o) of *Arabidopsis*. Boric acid treatment decreases Mg (a), Mn (c), Zn (e) and B (p) content but does not affect Ca (b) and Cu (d) contents in rosette leaves of *CsiLAC4^{OE}* lines. In the roots, boric acid treatment decreases Mg (f) and B (q) contents, but it results in the binding of more Ca (l), Mn (m), Cu (n) and Zn (o) in the cell walls of *CsiLAC4^{OE}* lines. Nutrient elements were determined by ICP-MS 14 d post the boric acid treatment. Results were mean \pm SD. ‘*’ indicates significant difference at $P < 0.05$ level by One-way ANOVA (S-N-K method, $n = 4$).

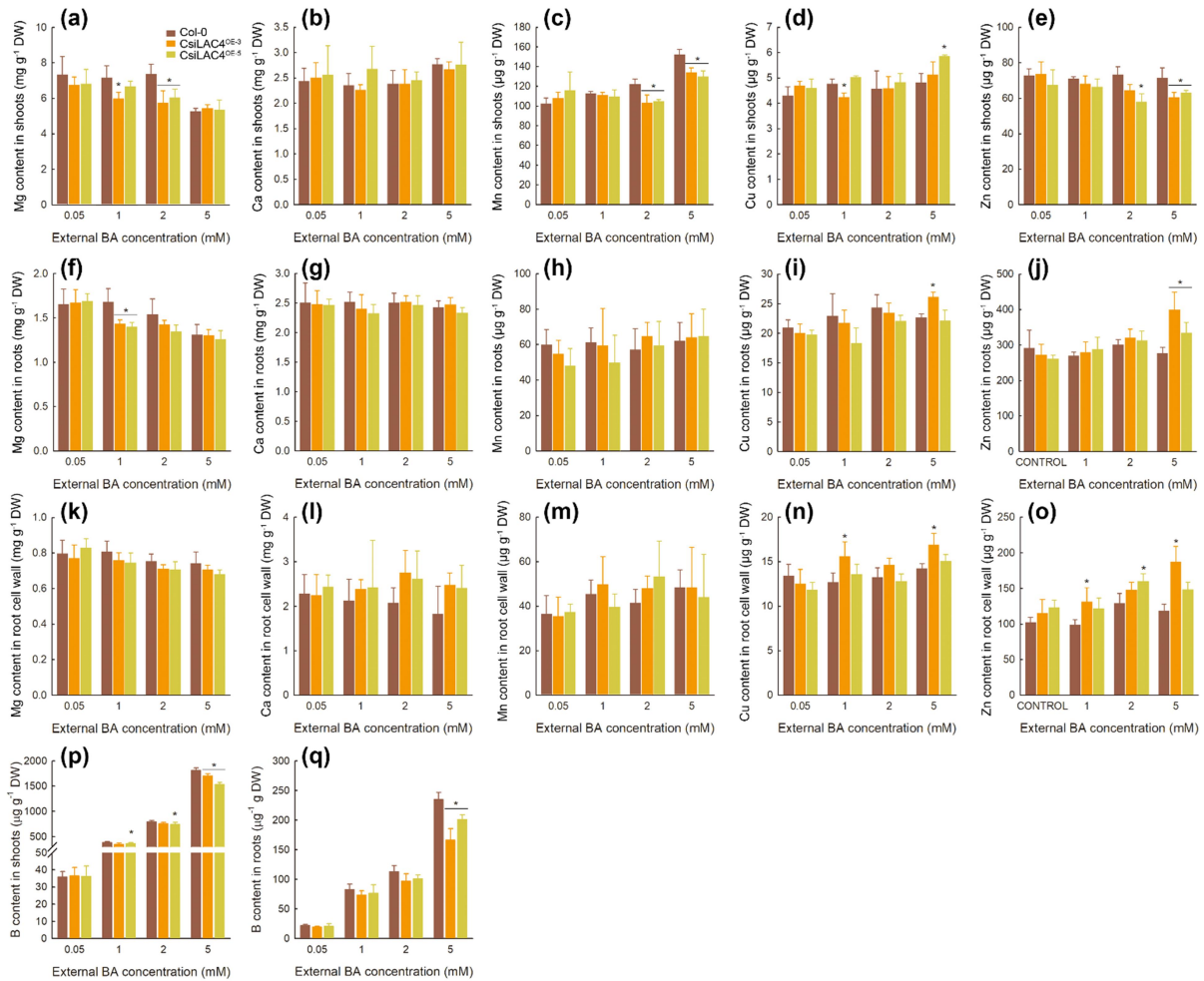


Table S1 Primers for PCR cloning of *pre-miR397*, *CsiLAC4*, *CsiLAC17*, and their corresponding probe template for *in situ* mRNA hybridization (ISH)

Genes	Primers	Sequence (5' - 3')
<i>Pre-miR397</i>	Forward	GGATCCATGGATCTGTTGCAGTTGAAACAAG
	Reverse	GAGCTCTTATTGACGATTGAGTCACAGAGGG
<i>CsiLAC4</i>	Forward	GGATCCATGGACTCCTGGGTTCCGGCTTCT
	Reverse	GAGCTCTTAACACTTTGGAAGATCACTTGGAGGT
<i>CsiLAC17</i>	Forward	GGATCCATGGGTGCTTCTCCGGCATTAAAT
	Reverse	GAGCTCTCAACACTTTGGAAGATCTGCCGGTG
<i>CsiLAC4-DsRed</i>	Forward	GGGACTCTTGCTGCAGGTATGGACTCCTGGGTTCCGGCTTCT
	Reverse	CGCGCCACTAGTGGATCCTACACTTTGGAAGATCACTTGGAGGT
<i>CsiLAC17-DsRed</i>	Forward	GGGACTCTTGCTGCAGGTATGGGTGCTTCTCCGGCATTAAAT
	Reverse	CGCGCCACTAGTGGATCCTACACTTTGGAAGATCTGCCGGTG
<i>miR397-ISH</i>	Forward	ATTTAGGTGACACTATAGAGCACTTGAAGATTCCCAGATTG
	Reverse	TAATACGACTCACTATAGGGAAAGAAACCTGTCAACCGTCAT
<i>CsiLAC4-ISH</i>	Forward	ATTTAGGTGACACTATAGCAACTCTCACCAGCACTCCT
	Reverse	TAATACGACTCACTATAGGGAGCCTGAAGCAACGCAATC
<i>CsiLAC17-ISH</i>	Forward	ATTTAGGTGACACTATAGGTTGTCGAAGTGGATGCTGTT
	Reverse	TAATACGACTCACTATAGGGTTGAGAGGTGGTAGGATTGGTT

Table S2 Primers for site-directed mutagenesis PCR of *CsiLAC4* and *CsiLAC17*

Primers	Sequence (5'-3')
<i>CsiLAC4*-F</i>	CCTACATGCTACGAATAATCAATGCTACCCTAACTGAAGAGCTA
<i>CsiLAC4*-R</i>	TTGATTATTCGTAGCATGTAGGTTTTGCCGCTGTCCACAGGCAATG
<i>CsiLAC17*-F</i>	AATTCTACCCTAACTGATGACCTCTTCTTCAGTATAGCAAAT
<i>CsiLAC17*-R</i>	GTCATCAGTTAGGGTAGAATTGACTAATCGGAGAAGGTAAGTTTT

Table S3 miRNA northern blotting probe

Probe	Sequence (5' - 3')
miR397	ATCAACGCTGCACTCAATGA
U6	AGGGGCCATGCTAATCTTCTC

Table S4 Specific and nested PCR primers for cleavage site validation

Primers	Sequence (5' - 3')
<i>CsiLAC17_GSP</i>	ATTGTAGCCATGCAAATGAAGAGG
Nested <i>CsiLAC17_GSP</i>	GTTTCTCATACTCTAAGATGCCAGC
<i>CsiLAC4_GSP</i>	TCATTAGGGCCTTTGCCATTGTCAACC
Nested <i>CsiLAC4_GSP</i>	TTGAATCCGTGTAAATGGACTGG

Table S5 Primers for qPCR of LACCASE-like family genes in *Citrus* and *Arabidopsis*

Primer	Sequence (5' - 3')
<i>β-actin-F(Citrus)</i>	AGAACTATGAACTGCCTGATGGC
<i>β-actin-R(Citrus)</i>	GCTTGGAGCAAGTGCTGTGATT
<i>Tubulin-F</i>	GCATCTTGAACCCGGTAC
<i>Tubulin-R</i>	ATCAATTCGGCGCCTTCAG
<i>Cs6g06880-F</i>	TGCTCAGCCAAAGATACATTCA
<i>Cs6g06880-R</i>	AGAAAGTGGCATTGTTGGGTAAGA
<i>Cs6g06920-F</i>	CAGGAAAGACATACCTCTTGAGAC
<i>Cs6g06920-R</i>	AGTGTCGAAAGGCTTGACG
<i>Cs8g 17350-F2</i>	ATTTATCGCCCTGTGTCTGCT
<i>Cs8g 17350-R2</i>	GACCTCCGTTGAACCACTCTC
<i>Cs8g17350-F (iso)</i>	CTTCAGCATAGCAAACCACACC
<i>Cs8g17350-R (iso)</i>	TTTCATACTCTAAGATACCAGCAACG
<i>Cs8g17630-F (CsiLAC17)</i>	CTTCTCCGATTAGTCAATTCTGC
<i>Cs8g17630-R (CsiLAC17)</i>	ATGACTAGCGTTTCGGTCTCAA
<i>Cs8g18800-F</i>	GAGGCAATTATCAATCAGTCTTTAC
<i>Cs8g18800-R</i>	GCTTCAACAACAGTGAGCGTA
<i>Cs7g23490-F</i>	AAACAGGAGGAGCACCGAATA
<i>Cs7g23490-R</i>	GTTGGCGTTAGGAGCCTTAGAT
<i>Cs6g06890-F</i>	TGGAGAATGGTGGAAAGCAGACA
<i>Cs6g06890-R</i>	GCAATTATACAAGGGACCAGGAAGA
<i>Cs6g11860-F</i>	CTCTTCCCTTGCTCTGAGAAA
<i>Cs6g11860-R</i>	CAAGAACATTTGTAGTTTGACCTG
<i>Cs1g24250-F</i>	CTTCTCTTTCTGCTACTTGGACTT
<i>Cs1g24250-R</i>	GCTAACATTCTTCACTTGAACATCG
<i>Cs7g31620-F</i>	TCAGGGCAGATAATCCAGGTGTT
<i>Cs7g31620-R</i>	CGTCGGAAGGTCCTAGGAGGAG
<i>Cs6g07800-F (CsiLAC4)</i>	CGTCACAGGGAGGCTTTACATT
<i>Cs6g07800-R (CsiLAC4)</i>	TGGTTTAACATAAGTGGCATCA
<i>Cs8g19850-F</i>	CGGGAAGACGTACATGCTGAG

<i>Cs8g19850-R</i>	TCAACGACTGTGAGTTTATGGC
<i>Cs8g11710-F</i>	TTGCTTTCGTGGCTTCTCTTTCT
<i>Cs8g11710-R</i>	CTCTTCACTGGCTTGGCTTCA
<i>Cs8g20850-T</i>	AAATGCTGCCTTTGACAATACC
<i>Cs8g20850-R</i>	CCATAGACCTCGGCTTACATTAC
<i>Cs7g30410-F</i>	CAAGCACATCACCACGGCAT
<i>Cs7g30410-R</i>	CTCCAACAGGCACACCAACG
<i>Cs6g07410-F</i>	GCTCTCAAATCAAACCTACACGC
<i>Cs6g07410-R</i>	GGTCCACCCTTTAATCCAGTCA
<i>Cs6g07400-F</i>	ATCCCTGCTCGGAAAATCAAA
<i>Cs6g07400-R</i>	CGTGTAGGCTGTAGGCGTATCA
<i>Cs6g07450-F</i>	GGAAGGGAAGACATATCTGCTAC
<i>Cs6g07450-R</i>	GACGTAGGGATCAGTGTAGGAA
<i>Orange1.lt00518-F</i>	TATGGCTATGCTTGTATTCTGTG
<i>Orange1.lt00518-R</i>	GACTGTGACGATGTCTTTGGC
<i>Cs3g22170-F</i>	GGCTTACTACGAACGCATCA
<i>Cs3g22170-R</i>	TTCCGAACCCAAATCCAAC
<i>Cs1g01800-F</i>	TTGAGTAACAAGACGAGTGAGACA
<i>Cs1g01800-R</i>	ATCCATAACGATGAACAGGCA
<i>Cs2g29090-F</i>	GGAAGAAAACCTGAAACCCCT
<i>Cs2g29090-R</i>	TGTTGGAGAATGATTTGCTGTG
<i>Cs7g21890-F</i>	TAGTAGTATTTACGGTGTTCGGG
<i>Cs7g21890-R</i>	CCTCTAATGTCCTTGGCTTGA
<i>Cs7g21880-F</i>	ATCGCATAGTCATTTCTGTCCC
<i>Cs7g21880-R</i>	TTGTAAGCCGTAAGTGAAGTGTT
<i>Orange1.lt01564-F</i>	GGCAGTTTCCAGGACCGAT
<i>Orange1.lt01564-R</i>	CCTTAGTTTCTTATGACTCTTCGT
<i>Cs9g14470-F</i>	ACCAAGTGACATTTACAACCAA
<i>Cs9g14470-R</i>	GAACCATAATGAAAAGAACCCT
<i>Cs5g09230-F</i>	AGAGAGCATCGGGCGGTTTCG
<i>Cs5g09230-R</i>	GAGCCGTGTGGTTCCTCGTGT
<i>Cs9g03540-F</i>	CTTTAGGATACAGGGTCACACG
<i>Cs9g03540-R</i>	CCATAATACTCCGCAAACCTCA
<i>Cs1g23090-F</i>	GGTCCTAGATTGGATGTGGTAA
<i>Cs1g23090-R</i>	TCAGAGTTGATGGGAAGTAAAAGT
<i>Cs2g02940-F</i>	TGCTGGGGATTTTACTGTGCT
<i>Cs2g02940-R</i>	CAAGATGAATGTCAAGGGCGG
<i>Cs2g21220-F</i>	ACTTATTCCTGTGCCCTTTGA
<i>Cs2g21220-R</i>	GTGTTAGCATTTGAACCCCGA
<i>Cs3g26900-F</i>	TTGGGTTGTCCGTATGGATGGAG
<i>Cs3g26900-R</i>	ATGACTTGGGATACACCTGAACG

<i>Cs8g01960-F</i>	CAGCCCCACAGGATTTCTAC
<i>Cs8g01960-R</i>	GTTTGGTCTTGGTCCACTTGC
<i>AtGAPDH2-F</i>	GTTTGTGTGTGGTTGAGTTC
<i>AtGAPDH2-R</i>	TTCAATGTTCCAGTTGCCAG
<i>AtUBQ5-F</i>	CTCCTTCTTTCTGGTAAACGT
<i>AtUBQ5-R</i>	GGTGCTAAGAAGAGGAAGAAT
<i>AthLAC17-F</i>	GTGCCAAACAACATCTCTCTCCA
<i>AthLAC17-R</i>	CCATCAGCCCAACCACTTCGTAA
<i>AthLAC4-F</i>	CTACGCACGAGAAGATGACAC
<i>AthLAC4-R</i>	ATGTGTAGACTTGACCAGGCT
stl-mi397-RT	GTCGTATCCAGTGCAGGGTCCGAGGTATTCGCACTGGATACGACATCAAC
miR397-Forward	GGTCTCATTGAGTGCAGCGTTG
Universal Reverse	GTGCAGGGTCCGAGGT

Table S6 Boron fractions in *Citrus* leaves treated with different B treatments. Results were mean \pm SD. Different small letters in the same column indicated significant differences at $P < 0.05$ level (One-way ANOVA).

		Water-soluble B ($\mu\text{g g}^{-1}$, FW)	Organic-bound B ($\mu\text{g g}^{-1}$, FW)	Cell wall-bound B ($\mu\text{g g}^{-1}$, FW)
<i>C. sinensis</i>	Control	4.66 \pm 1.42 ^b	4.33 \pm 0.81	5.06 \pm 0.61
	B-toxicity	180.65 \pm 12.52 ^a	4.51 \pm 0.65	5.62 \pm 1.08
<i>C. grandis</i>	Control	4.13 \pm 1.01 ^b	3.65 \pm 0.97	5.33 \pm 0.83
	B-toxicity	174 \pm 10.18 ^a	4.30 \pm 0.45	4.98 \pm 0.77